

REPORT DOCUMENTATION PAGE				Form Approved OMB No. 0704-0188	
Public reporting burden for this collection of information is estimated to average 1 hour per response, including the time for reviewing instructions, searching existing data sources, gathering and maintaining the data needed, and completing and reviewing this collection of information. Send comments regarding this burden estimate or any other aspect of this collection of information, including suggestions for reducing this burden to Department of Defense, Washington Headquarters Services, Directorate for Information Operations and Reports (0704-0188), 1215 Jefferson Davis Highway, Suite 1204, Arlington, VA 22202-4302. Respondents should be aware that notwithstanding any other provision of law, no person shall be subject to any penalty for failing to comply with a collection of information if it does not display a currently valid OMB control number. PLEASE DO NOT RETURN YOUR FORM TO THE ABOVE ADDRESS.					
1. REPORT DATE (DD-MM-YYYY) 10-06-2008		2. REPORT TYPE Technical Paper		3. DATES COVERED (From - To)	
4. TITLE AND SUBTITLE The Pulse Detonation Rocket Induced MHD Ejector (PDRIME) Concept (Preprint)				5a. CONTRACT NUMBER	
				5b. GRANT NUMBER	
				5c. PROGRAM ELEMENT NUMBER	
6. AUTHOR(S) Jean-Luc Cambier (AFRL/RZSA); Timothy Roth, Christopher Zeineh, & Ann R. Karagozian (UCLA)				5d. PROJECT NUMBER	
				5e. TASK NUMBER	
				5f. WORK UNIT NUMBER 50260542	
7. PERFORMING ORGANIZATION NAME(S) AND ADDRESS(ES) Air Force Research Laboratory (AFMC) AFRL/RZSA 10 E. Saturn Blvd. Edwards AFB CA 93524-7680				8. PERFORMING ORGANIZATION REPORT NUMBER AFRL-RZ-ED-TP-2008-215	
9. SPONSORING / MONITORING AGENCY NAME(S) AND ADDRESS(ES) Air Force Research Laboratory (AFMC) AFRL/RZS 5 Pollux Drive Edwards AFB CA 93524-7048				10. SPONSOR/MONITOR'S ACRONYM(S)	
				11. SPONSOR/MONITOR'S NUMBER(S) AFRL-RZ-ED-TP-2008-215	
12. DISTRIBUTION / AVAILABILITY STATEMENT Approved for public release; distribution unlimited (PA #08236A).					
13. SUPPLEMENTARY NOTES For presentation at the 44 th AIAA Joint Propulsion Conference, Hartford, CT, 20-23 July 2008.					
14. ABSTRACT Pulse detonation engines (PDEs) have received significant attention due to their potentially superior performance over constant pressure engines. However due to the unsteady chamber pressure, the PDE system will either be over- or under-expanded for the majority of the cycle, with substantial performance loss in atmospheric flight applications. Thrust augmentation, such as PDE-ejector configurations, can potentially alleviate this problem. Here, we study the potential benefits of using Magneto-hydrodynamic (MHD) augmentation by extracting energy from a Pulse Detonation Rocket Engine (PDRE) and applying it to a separate stream. In this PDRE-MHD Ejector (PDRIME) concept, the energy extracted from a generator in the nozzle is applied directly to a by-pass air stream through an MHD accelerator. The air stream is first shocked and raised to high-temperature, allowing thermal ionization to occur after appropriate seeding. The shock-processing of the high-speed air stream is accomplished by using the high initial PDRE nozzle pressures of the under-expanded phase. Thus, energy could be efficiently transferred from one stream to another. The present simulations involve use of a simple blowdown model for PDE behavior, coupled to quasi-1D and 2D numerical simulations of flow and MHD processes in the rest of the PDRIME configuration. Results show potential performance gains but some challenges associated with achieving these gains.					
15. SUBJECT TERMS					
16. SECURITY CLASSIFICATION OF:			17. LIMITATION OF ABSTRACT SAR	18. NUMBER OF PAGES 23	19a. NAME OF RESPONSIBLE PERSON Dr. Jean-Luc Cambier
a. REPORT Unclassified	b. ABSTRACT Unclassified	c. THIS PAGE Unclassified			19b. TELEPHONE NUMBER (include area code) N/A

The Pulse Detonation Rocket Induced MHD Ejector (PDRIME) Concept

Jean-Luc Cambier*

Air Force Research Laboratory, Aerophysics Branch, Edwards AFB, CA 93524

Timothy Roth[†], Christopher Zeineh[‡], and Ann R. Karagozian[§]

Department of Mechanical and Aerospace Engineering, UCLA, Los Angeles, CA 90095-1597

Pulse detonation engines (PDEs) have received significant attention due to their potentially superior performance over constant pressure engines. However due to the unsteady chamber pressure, the PDE system will either be over- or under-expanded for the majority of the cycle, with substantial performance loss in atmospheric flight applications. Thrust augmentation, such as PDE-ejector configurations, can potentially alleviate this problem. Here, we study the potential benefits of using Magneto-hydrodynamic (MHD) augmentation by extracting energy from a Pulse Detonation Rocket Engine (PDRE) and applying it to a separate stream. In this PDRE-MHD Ejector (PDRIME) concept, the energy extracted from a generator in the nozzle is applied directly to a by-pass air stream through an MHD accelerator. The air stream is first shocked and raised to high-temperature, allowing thermal ionization to occur after appropriate seeding. The shock-processing of the high-speed air stream is accomplished by using the high initial PDRE nozzle pressures of the under-expanded phase. Thus, energy could be efficiently transferred from one stream to another. The present simulations involve use of a simple blowdown model for PDE behavior, coupled to quasi-1D and 2D numerical simulations of flow and MHD processes in the rest of the PDRIME configuration. Results show potential performance gains but some challenges associated with achieving these gains.

Nomenclature

A	=	Cross-sectional area
B	=	Magnetic field
c	=	Speed of sound
\vec{E}	=	Electric field
E, \hat{E}	=	Energy
F_L	=	Lorenz force
Re_m	=	Magnetic Reynolds Number
I	=	Impulse
j	=	Current density
\dot{m}	=	Mass flux
p	=	Pressure
T	=	Thrust
u	=	Velocity
x, y, z	=	Streamwise, transverse, and axial coordinates
γ	=	Ratio of specific heats
ρ	=	Density
σ	=	Electrical conductivity

* Senior Scientist, AFRL/RZSA

[†] Graduate Student Researcher; currently Member of the Technical Staff, Northrop-Grumman Space Technology

[‡] Graduate Student Researcher

[§] Professor, AIAA Fellow; corresponding author (ark@seas.ucla.edu)

PREPRINT

Introduction

Robust propulsion systems for advanced high speed air breathing and rocket vehicles are critical to the future of Air Force missions, including those for global/responsive strike and assured access to space. A novel combined cycle propulsive concept, the Pulse Detonation Rocket-Induced MHD Ejector (PDRIME) proposed by Cambier¹, is one of a number of alternative magneto-hydrodynamic (MHD) augmentation ideas that shows promise for application to a wide range of advanced propulsion systems. Taking advantage of the unsteady engine cycle associated with the pulse detonation rocket engine (PDRE), PDRIME involves periodic temporal energy bypass to a seeded airstream, with MHD acceleration of the airstream for thrust enhancement and control. The range of alternative MHD-augmented propulsion configurations that could be employed suggests that the PDRIME type of concept could be applied to hypersonic air-breathing systems, space power production for directed energy weapons (DEW) and remote sensing systems, electromagnetic countermeasures, and other potential Air Force systems for the mid-to-far term.

Background: Conventional Rocket Systems and PDREs

Chemical rocket engines store both fuel and oxidizer, unlike air-breathing engines which utilize the oxygen in air in the combustion process. Liquid rockets typically employ a constant pressure reaction, where reactants are continually fed at high pressure into the combustion chamber. Rocket engines typically use a converging-diverging (Laval) nozzle to expand the flow and convert the high pressure and temperature of the propellants into thrust. Properties of a nozzle flow depend strongly on the pressure upstream (inside the combustion chamber, P_c), and at ambient (p_a), downstream of the nozzle exit, as well as the exit-to-throat area ratio for the nozzle, A_e/A^* . The thrust generated by a rocket is typically expressed as:

$$T = \dot{m}V_e + (p_e - p_a)A_e \quad (1)$$

where \dot{m} is the mass flux of gas exiting the nozzle, V_e is the exhaust velocity, and p_e is the pressure at the exhaust of the nozzle.

The maximum thrust² occurs when the propellants are expanded to the point where the pressure at the exit of the nozzle is equal to the ambient pressure. Further expansion of the gas in the nozzle will reduce the thrust, as the ambient pressure will then exceed the exhaust pressure, creating pressure drag. This added drag can outweigh momentum gains arising from the further acceleration of the flow from the nozzle, i.e., the increase in exhaust velocity. Under-expansion in the nozzle will result in lower than optimal thrust as the maximum momentum gains are not realized. Another performance parameter, impulse I , is the thrust integrated over time t :

$$I \equiv \int T(\tau) d\tau \quad (2)$$

Another common performance parameter, specific impulse I_{sp} , is the impulse divided by the weight of the reactants or propellants.

One alternative configuration to the traditional rocket engine which has the potential for operating as a constant volume cycle, and hence could be theoretically more efficient, is the pulse detonation engine or PDE (a subset of which is the pulse detonation rocket engine or PDRE). The pulse detonation engine operates in a cycle. Reactants are added to the combustion chamber at low pressure, and are mixed. The mixture is ignited and a detonation wave propagates across the chamber. This detonation raises the propellants to high pressure and temperature, and can be modeled as a constant volume reaction, which is more efficient than a constant pressure reaction. After the detonation wave (or shock wave, after reactants have been consumed) exits the nozzle, an expansion wave is reflected back into the nozzle and eventually propagates into the chamber. The expansion wave thus lowers the overall pressure throughout the chamber, and upon reflection at the thrust wall, the lowered pressure allows reactants to be drawn into the chamber. The reflection of the expansion wave at the nozzle exit results in a reflected compression wave, which is strengthened and becomes a shock. When the shock reflects at the thrust wall, the reactants in the chamber can be ignited, and the ignition of the detonation wave starts the process once again. A number of recent studies have explored the nature and performance characteristics of PDEs of various geometries^{3,4,5,6,7,8}. The PDE was even recently tested for the first time in flight on a Scaled Composites Long EZ aircraft⁹, with four PDE tubes operating at a cycle frequency of 20 Hz.

In the past, our group at UCLA^{10,11} has explored the influence of PDE geometry, reaction kinetics, and flow processes using high order numerical methods. A fifth-order WENO (weighted essentially non-oscillatory^{12,13}) scheme was used for spatial integration of the reactive Euler equations, with a 3rd-order Runge-Kutta time

integration in the case of simplified reaction kinetics; a stiff ODE solver was used for temporal integration in complex kinetics simulations. While the simulations using complex kinetics provide useful quantitative data, the simulations with reduced kinetics (a single step reaction) in fact can provide very similar quantitative performance results.

In general, two different methods could be used to generate thrust from PDREs. The first involves a straight or slightly contoured nozzle. The main goal of this configuration is to exploit the thrust generation from the ignition of the detonation wave near the thrust wall and the propagation of the detonation wave through the device, as described above. The second approach is more similar to a constant-pressure rocket. Here the nozzle throat is small enough to prevent the main detonation wave to escape the chamber. This creates multiple reflected compressive waves in the chamber; which homogenize the chamber pressurization, resulting in an approximately constant volume reaction. During the blow-down period the reactants are driven out from the chamber and through the nozzle. Similar to the constant-pressure rocket, the exhaust gases are expanded, increasing the velocity and reducing the pressure. The difference between this type of PDRE and a constant-pressure rocket is that in the PDRE, the chamber pressure is decreasing throughout the blow-down period as mass is ejected from the chamber with no immediate replacement. New reactants are added to the combustion chamber once the pressure has been reduced to a specified value and then the cycle is repeated.

Due to the unsteady nature of the chamber pressure, however, a PDRE nozzle can only be perfectly expanded briefly within a blow-down period. This implies suboptimal use of energy to attain this condition for most of the cycle. At low altitudes, nozzles with large area ratios are subject to large drag forces ($P_a > P_e$), while nozzles with relatively smaller exit areas will be under-expanded for the majority of blow-down.

The PDRIME Concept

Ejectors are often used to transfer energy from one stream to another stream, providing an additional source of thrust, especially for an air-breathing engine. Ejectors have been shown to produce overall thrust gains when energy is being taken from a high velocity flow and transferred to a low energy stream, in the ejector, with a high mass flow rate. In the present application for the PDRE, energy can be extracted from the nozzle when the marginal decreases in thrust are small and added to a bypass air flow, to assist in augmentation of the thrust. Ejectors typically transfer energy between streams through shear stress between separate flow streams. A portion of the main flow is diverted into a channel to mix with the lower velocity flow. The drawback of this method is that the ability to transfer energy is limited by the contact area between the two streams. At large velocities shear layer thicknesses are small, leading to the necessity for large channels for mixing, which add weight.

In contrast, if magnetohydrodynamic (MHD) forces are applied as body forces to the ejector flow, affecting the entire field immediately, there can be substantial benefits. This could reduce the length of the bypass tube and time necessary for complete energy transfer as well as providing the flexibility of energy extraction and application, since the applied fields can be varied.

Our possible configuration attaches a converging-diverging nozzle to the combustion chamber of a PDRE with a bypass tube. A generic configuration for this concept, called the Pulse Detonation Rocket Induced MHD Ejector, is shown in **Figure 1**. Magnetohydrodynamics (MHD) describes the interaction between a magnetic field and an electrically conducting fluid flow. For the present applications, magnetic and electric fields are applied both normal to each other, in the z and y direction respectively, and normal to the fluid velocities (in the nozzle and bypass-tube, the x -direction).

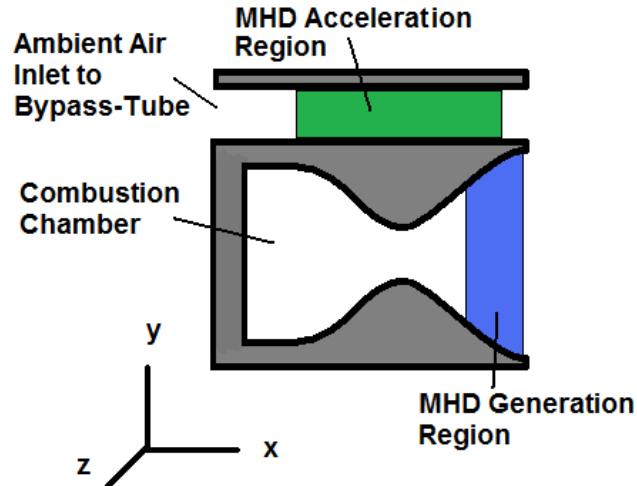


Figure 1: The generic PDRIME configuration, indicating the PDRE combustion chamber and regions in which MHD generation/extraction and flow acceleration in a bypass section take place.

In the expanding (divergent) section of the nozzle, magnetic and electric fields are applied to extract energy from this portion of the flow. A bypass-tube sits adjacent to the engine. Ambient air enters this tube and is accelerated by an MHD accelerator powered by the energy extracted from the nozzle. A gain in thrust is realized by extracting energy from the nozzle, which would otherwise be used inefficiently, and by applying the energy to the air in the bypass-tube. A planar design is used to achieve a spatially uniform magnetic field, only in the z -direction, by placement of magnets above and below each region.

More details on the evolution of the flow cycle for the PDRIME are shown in **Figures 2a and 2b**. Because a PDRE can be designed to have a converging-diverging nozzle such that the initial peak pressure in the combustion chamber results in a pressure at the nozzle exit plane that is well above ambient, a shock structure (locally oblique) is exhausted at the nozzle lip, indicated in **Fig. 2a**. Consistent with the Rocket-Induced MHD Ejector (RIME) concept¹⁴, the shock produced at the PDRE's nozzle exit can potentially enter the bypass channel, traveling upstream. If the air is initially at high Mach number in the bypass channel, this traveling shock brings the air to a high temperature at which a high conductivity species such as Cesium can be added to the flow, thus increasing the conductivity of the air. Hence the shock generates a slowly-moving slug of high-temperature air that can be more easily ionized.

As the pressure at the nozzle exit drops during blow-down, the shock then slows down, and eventually the ionized air starts to move downstream. At this point, electrical power can be applied to accelerate the air slug from the bypass tube and thus generating thrust (**Figure 2b**). The procedure can then be repeated at each cycle. One only needs to design the nozzle such that the flow is under-expanded during the initial part of the blow-down phase. In fact, there may be a self-adjusting process at work, depending on PDRE nozzle design and altitude as outlined by Cambier¹. While at launch, the nozzle exit pressure is equal to ambient and there is no interaction with the bypass air, as the vehicle accelerates and gains altitude, the nozzle becomes progressively under-expanded, so that eventually a strong shock can be generated for the bypass channel to ionize the seeded air, and the ejector operates. This is one of several configurations in which the PDRIME concept could be used for thrust augmentation in advanced propulsion systems.

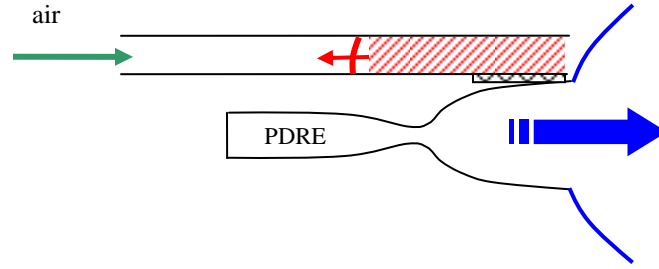


Figure 2a: Schematic of the PDRIME concept during the initial portion of the cycle. Overpressure at the nozzle exit blocks flow in the bypass channel. An upstream propagating shock slows and raises the temperature of the seeded air in the bypass channel.

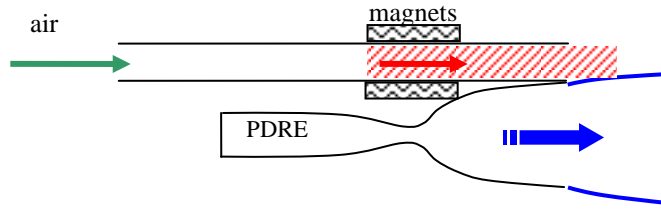


Figure 2b: Schematic of the PDRIME concept during the latter part of the cycle, during blow-down. As the pressure at the nozzle exit drops, exit of the compressed and heated air from the bypass channel takes place. Power is applied during the MHD acceleration of the air slug.

As noted above, the MHD “generator” is located in the diverging section of the nozzle where the velocity is largest, so that the expansion of the fluid counteracts some of the velocity reduction arising from the Lorentz (“drag”) force acting in the generator. The Lorentz force acts on all conductors carrying a current in a magnetic field. This is given in general by

$$\vec{F}_L = \vec{j} \times \vec{B} \quad (3a)$$

or, for the current orientation of vectors:

$$F_{L,x} = j_y \times B_z \quad (3b)$$

An important property of the MHD flow system is the current density, \vec{j} , which is related to electric and magnetic fields, \vec{E} and \vec{B} , via Ohm’s law:

$$\vec{j} = \sigma(\vec{E} + \vec{u} \times \vec{B}) \quad (4)$$

where σ is the electrical conductivity (with units of Mho). For the PDRIME orientation described in **Figure 1**, this reduces to a current density with a component in the y-direction only:

$$j_y = \sigma(E_y + u_x \times B_z) \quad (5)$$

where E_y is the electric field acting in the y-direction and B_z is the magnetic field acting in the z-direction. A Magnetic Reynolds number, R_m , is a dimensionless parameter which indicates the magnitude of these interactions:

$$R_m = \mu\sigma uL \quad (6)$$

where μ is the permeability of free space (units of N/A^2), u the velocity and L is a characteristic length scale. The motion of the electrically conducting fluid induces an additional magnetic field, but for low Magnetic Reynolds numbers, this is negligible and the magnetic field may be considered constant. A low Magnetic Reynolds number approximation is assumed for our MHD applications.

Note that with a constant and positive magnetic field, the direction of the Lorentz force depends on the relative magnitudes of E_y and $u_x \times B_z$ from eqn. (5). We designate a loading factor, K_y , to compare these strengths:

$$K_y = \frac{E}{u \times B} \quad (7)$$

When K_y is less than unity, the current density in the y-direction is negative, resulting in a Lorentz force opposing the fluid motion. Energy effects of MHD application are governed by the current density multiplied by the electric field. This can be decomposed into two terms:

$$\vec{j} \cdot \vec{E} = \frac{\vec{j}^2}{\sigma} + \vec{u} \cdot (\vec{j} \times \vec{B}) \quad (8)$$

where the terms on the right hand side represent the dissipative heating and mechanical power, respectively. When the loading factor K_y is less than 1, the mechanical power is negative because energy is being extracted from the fluid. Thus in the PDRIME configuration, for MHD generation in the nozzle, the loading factor is less than 1, causing energy to be extracted from the fluid in the nozzle, with a negative Lorentz force. In the accelerator (bypass section), a positive Lorentz force and application of energy takes place. Regardless of the loading factor, the joule heating will always be a positive term, representing a loss in both cases. Ignoring dissipative effects, we see that the Lorentz force scales with velocity, while the energy associated with both generation and acceleration scales with velocity squared. For this reason, maximum thrust gain is achieved when energy is extracted from high velocity flows, as in the nozzle, and applied to low velocity flows.

The optimal loading factor K_y for MHD generation is shown by Cambier¹³ to be 0.5. For $K_y < 1$, the goal is to extract maximum power ($\sim K_y$) with minimal dissipation ($\sim K_y^2$). The energy generated in the nozzle is then applied in the bypass-tube by a MHD accelerator. Further information on the loading factor will be provided in a later section.

The goal of the present research involves use of a simplified model for the blow-down portion of the PDRE, coupled to a more detailed simulation of the relevant MHD processes in the nozzle and/or adjacent bypass sections, as a means of predicting overall PDRIME phenomena and performance parameters. The model is validated using detailed numerical simulations of PDRE processes, so that projections for optimal performance and operating conditions may be made.

Description of the PDRIME Model and Simulation Procedure

Model Framework

Due to the large number of available system parameters in the PDRIME, a rapid simulation technique is required, one that is simpler than a detailed numerical simulation of flow and reactive processes in the PDRE and adjacent flow sections. Detonations constitute a major computational cost. The sharp gradients and large sound speeds present in the PDE greatly reduce the time-step and require finer spatial resolution^{15,16}. After the shock waves have subsided in the combustion chamber, the properties of the fluid within the combustion chamber are mostly uniform, resembling the products of a constant volume reaction. For these reasons a blow-down model was developed by Cambier¹⁷ to predict chamber properties as a function of time after a constant volume reaction. This blow-down model is in a single cell which represents the entire PDE combustion chamber. The converging section of the nozzle is also represented by a single cell approximation. An adiabatic solution for the throat conditions for every time-step is determined based on the combustion chamber properties and the assumption that the throat is choked. The divergent section, throat to exit, is fully discretized, as is the entire bypass-tube. In order to validate certain aspects of the engine cycle and flow processes, comparisons with full 2D transient numerical simulations are also made.

Description of Blow-down Model

The PDE cycle begins when the combustion chamber is full of reactants. An external spark then sends a detonation wave through the combustion chamber, raising the pressure of the propellants. The pressure difference between the combustion chamber and the ambient air drives the propellants out of the combustion chamber, representing the blow-down process. The presence of a nozzle changes the blow-down profile. Intuitively, a smaller throat, which restricts the mass flow of propellants out of the chamber, will lead to a slower decay, increasing the blow-down period. With small enough throat areas, the constant pressure period following the PDE's detonation becomes negligible, and only blow-down needs to be considered for thrust calculations. Here the reaction is approximated as a constant volume reaction.

PREPRINT

To predict this pressure decay inside the combustion chamber a simple model developed by Cambier is used. This model starts with the combustion chamber filled with post-constant volume reaction products at high pressure and temperature. The mass and energy flow rate of the products through the throat are then calculated based on current conditions:

$$\frac{dM}{dt} = -\dot{m} = -\Gamma \rho_o c_o A^* \quad (9)$$

$$\frac{dE}{dt} = -\dot{m} \cdot h_o = -\dot{m} \cdot C_p T_o \quad (10)$$

where

$$\Gamma = \left(\frac{2}{\gamma + 1} \right)^{\frac{\gamma + 1}{2(\gamma + 1)}} \quad (11)$$

and ρ_o is the density of the products, A^* is the area of the choked throat, c_o is the sound speed, h_o is enthalpy, and C_p is the heat capacity at constant pressure. The volume is constant, thus equation (9) reduces to a partial differential equation defining the behavior of density in the combustion chamber. Blow-down is an adiabatic process, and for high temperature water vapor (products), $\gamma \sim 1.2$. The system (9-10) yields a differential equation for the stagnation temperature which can be analytically solved for constant γ . Instead, we solve the system numerically and update γ, Γ using the true caloric EOS at each time step. In this approach the entire combustion chamber is represented with a single cell, greatly reducing computational time.

Discretization of Nozzle and Bypass Sections

The diverging section of the nozzle and the bypass-tube are divided into cells. The quasi-1D equations which govern this flow in conservative form are similar to those in He and Karagozian⁸ but without the species terms and with the inclusion of momentum and energy source terms corresponding to MHD effects:

$$\frac{\partial (AU)}{\partial t} + \frac{\partial (F_x(U))}{\partial x} = \frac{dA}{dx} H + AS(U) \quad (12)$$

$$U = \begin{pmatrix} \rho \\ \rho u \\ \hat{E} \end{pmatrix}, F_x(U) = \begin{pmatrix} \rho u \\ \rho u^2 + p \\ (\hat{E} + p)u \end{pmatrix}, H = \begin{pmatrix} 0 \\ p \\ 0 \end{pmatrix}, S(U) = \begin{pmatrix} 0 \\ j_y \times B_z \\ j_y \cdot E_y \end{pmatrix} \quad (13)$$

$$\hat{E} = \frac{p}{\gamma - 1} + \frac{\rho u^2}{2} \quad (14)$$

where $A(x)$ is the cross-sectional area as a function of position, and \hat{E} is energy.

To further streamline this rapid simulation, the flow inside the diverging section of the nozzle is modeled using a quasi-steady solution to these equations. This is valid when the characteristic time scale of the flow in the nozzle with the small throat is much shorter than the blow-down time scale of the chamber. First the governing equations are rewritten in primitive form:

$$\frac{1}{\rho} \frac{d\rho}{dx} + \frac{1}{u} \frac{du}{dx} + \frac{1}{A} \frac{dA}{dx} = 0 \quad (15)$$

$$\frac{dp}{dx} + \rho u \frac{du}{dx} = j_y \times B_z \quad (16)$$

$$\frac{\gamma}{\gamma - 1} \rho u \frac{d}{dx} \left(\frac{p}{\rho} \right) + \rho u^2 \frac{du}{dx} = j_y \cdot E_y \quad (17)$$

These equations are then normalized and solved with a forward marching scheme, starting with the throat conditions and marching to the exit. The flow is supersonic everywhere in the diverging section of the nozzle, which allows for the quasi-steady forward-marching scheme to be employed. Since this model is quasi-steady, there is no numerical

time integration, though the time-step between applications of the model is still limited by the speed of sound in the combustion chamber.

When the pressure at the exit reaches a low enough level, a shock will propagate into the nozzle. The forward-marching scheme has no way to detect this condition, hence a separate check of the conditions at the exit is performed. When a shock enters the nozzle, it reduces the local exit velocity and raises the pressure at the exit to become equal to the ambient fluid exterior to the nozzle; the former phenomenon reduces thrust and the latter phenomenon reduces the drag. Simulating for additional time beyond this condition will not change the total impulse calculated for the cycle and hence is not necessary.

Transient flow in the bypass-tube involves a shock created by the nozzle exhaust, traveling into the bypass exit and propagating to the left into a high speed right-moving flow. Quasi-steady forward-marching methods are thus not adequate for these regimes, especially since this method has a singularity when the flow Mach number is equal to one. For these reasons, a fully transient numerical scheme must be used to simulate flow in the bypass-tube.

In simulating flow in the bypass-tube, the Weighted Essentially Non-Oscillatory (WENO) method¹³ is used to approximate spatial derivatives, with a stencil including upstream and downstream cells. This is an adaptation of the Essentially Non-Oscillatory (ENO) method^{12,18} which uses the conservation laws for high order accuracy with shock capturing capabilities. Artificial viscosity is added via the Local Lax Friedrich (LLF) scheme to avoid entropy violation and reduce dispersion. Temporal integration is performed by a 3rd order Runge-Kutta method, which uses an internally iterative process to achieve fairly large time-steps without loss of high order accuracy. The time-step is regulated by the Courant-Friedrichs-Levy (CFL) condition, which ensures stability by limiting the time-step to a ratio of the cell lengths and sound speeds.

Integration of Model Components

The computation of flow in the combustion chamber and nozzle constituting the PDE is decoupled from that in the bypass-tube. The PDE system simulation does not require input from the bypass-tube simulation and will be discussed first. No components of the engine system have dependence on past time-steps using Cambier's blow-down model. This cycle starts with the initiation of blow-down and ends when combustion chamber pressure reaches a prescribed value. At a given time the combustion chamber properties are calculated by the blow-down model, which is only a function of time and system parameters. The conditions in the throat are then determined based on chamber properties. The flow in the diverging section of the nozzle is then found by marching forward from the throat, where the properties are known, to the exit. The maximum allowable time-step is then calculated; time is increased, and the blow-down model again calculates combustion chamber properties. The cycle continues until the chamber pressure is reduced far enough or until shock conditions are detected.

Each cycle may be simulated for specific ambient conditions dictated by altitude. For the engine system, altitude affects pressure downstream of the nozzle, and changes the thrust calculated by equation (1), via changes in P_a . The PDE code thus stores exit pressure and Mach number as a function of time, as well as total impulse and energy extracted for every altitude and engine system configuration. The bypass-tube is then employed and coupled with a specific engine system simulation. The bypass model is run using the specified altitude to determine inlet conditions. The exit pressure from the PDE system is used as a time dependent boundary condition for the downstream end of the bypass-tube. The energy applied in the bypass-tube to accelerate the air is limited to the energy extracted from the engine system. At the end, the net impulse arising from flow in both systems over one cycle is found. The speed at which the vehicle travels is the only independent variable in the bypass-tube and dictates the inlet velocity or Mach number.

Two-Dimensional Transient Simulations

As a means of validating many of the assumptions that enter in to the quasi-1D simulations of the PDRIME configuration, corresponding simulations of two-dimensional flow in the nozzle, bypass tube, and exterior region have been conducted by Zeineh¹⁹. These simulations employ a simplified representation of the blow-down process as done in the present modeling, but then employ a 5th order WENO simulation, as done in He and Karagozian^{10,11}, to resolve the flow beyond the nozzle throat and exterior to the PDRIME. This allows assumptions pertaining to the transmission of the shock from the nozzle to the bypass tube, for example, to be validated.

Model Validation

This section shows the steps taken to ensure that, despite the many simplifications utilized in these simulations, the results reasonably accurately reflect the performance of a PDRIME system. Thrust estimation from flow properties may be derived from the momentum fluxes in the problem. For PDREs, the contributions of the transient term in the momentum conservation equation are observed to be negligible, a result of the blow-down approximation with a small throat area.

As noted previously, to reduce computational costs the present model represents the PDE cycle by a constant volume reaction followed by a blow-down period. The validity of this model depends on the throat cross-sectional area. A large throat area will allow propellants to leave the combustion chamber as the detonation wave propagates through it, hence this will not produce a constant volume reaction. A smaller throat area (compared with the cross-sectional area of the chamber) can limit the amount of mass which escapes until the reflected waves have brought the products in the combustion chamber to conditions resembling the result of a constant volume reaction. Cambier¹⁷ demonstrated that the aforementioned simple blow-down model (with a constant volume reaction) can produce nearly the same computed impulse for the actual pulse detonation reaction with a nozzle, with chamber-to-throat area ratio of 16. The comparison is accomplished by closing the throat in the PDE computation until the reaction has gone to completion and then allowing the reactants to escape. The full quasi-1D PDE cycle starts with reactants being ignited by a detonation wave, whose evolution is simulated numerically using a 4th order piecewise parabolic method (PPM). These two different methods show good agreement and have consistent trends, hence the present exploration incorporates the Cambier blow-down model in its PDRIME simulations.

Comparison of the simple blow-down model and a quasi 1D, transient numerical simulation of blow-down may also be conducted. **Figure 3** plots pressure as a function of time at the closed wall (left end) of the combustion chamber and also in the middle of the combustion chamber, using the quasi-1D numerical simulation described previously, with WENO for spatial discretization and Runge-Kutta time integration. Pressure at the single “chamber” cell represented in the simple blow-down model is also plotted for comparison. Again, the blow-down model shows good agreement with the detailed quasi-1D numerical simulation. In addition, the similar values of pressure at different locations (thrust wall and center of chamber) show uniformity within the combustion chamber. The slight offset in time between the blow-down model and the full numerical simulation can be attributed to the time required for the constant volume reaction to complete. This model neglects this time and starts blow-down immediately.

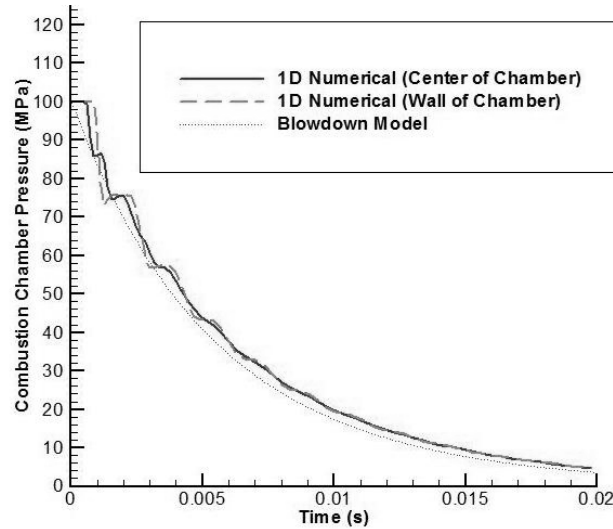


Figure 3: Pressure (MPa) versus time (units of seconds) for two different locations in the combustion chamber, at the thrust wall and in the center of the chamber, derived using the numerical, quasi 1D spatially resolved model and the blow-down model.

The adiabatic calculation which approximates the conditions at the nozzle throat, based on the combustion chamber properties, is also validated using a quasi-1D numerical code. **Figure 4** also shows consistency between the WENO simulation and the rapid blow-down model, but again with a slight time lag. This provides us with confidence in replacing the entire numerical domain for the PDE, from combustion chamber to the nozzle throat, with the simplified blow-down model, which provides similar results at a fraction of the computational demand.

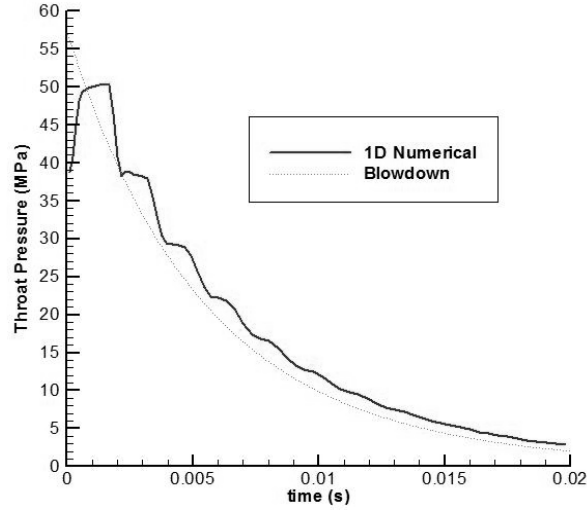


Figure 4 Throat pressure (MPa) as a function of time (s), derived using the numerical, quasi 1D spatially resolved model and the blow-down model.

We finally note that use of a quasi-1D simulation for flow processes associated with a PDE with a nozzle, as compared with results from a fully 2D transient code; yield very similar results for relatively low exit-to-throat nozzle ratios (He and Karagozian¹¹). Hence both the blow-down model and quasi-1D portions of the simulation should represent the PDRIME concept quite well.

Results and Performance Evaluation

MHD Energy Generation/Extraction versus Thrust Lost

This section first focuses only on resolving phenomena for the PDE, that is, in the combustion chamber and nozzle. The results of this system are hence independent of the presence of bypass-tube. The impulse and thrust of this system are shown with and without MHD generation to compare the net result of MHD energy extraction from the nozzle on device performance. Extracted energy is quantified as well as nozzle exit pressure as a function of time, to be used as inputs to the bypass-tube computations.

As an example of conditions for PDE operation using the blow-down model, the cycle starts with water vapor products in the combustion chamber at a pressure and temperature of 100atm and 3000K, respectively. The cycle is first assumed to operate at an altitude of 10km and has an exit-to-throat ratio of 35. A magnetic field is uniformly applied (spatially) across the rear half of the diverging section. The strength of the magnetic field is varied with time to maximize energy extraction while keeping the flow at the exit supersonic, at a specified Mach number of 1.2. For this cycle the strength of the applied magnetic field, B as a function of time is shown in **Figure 5**.

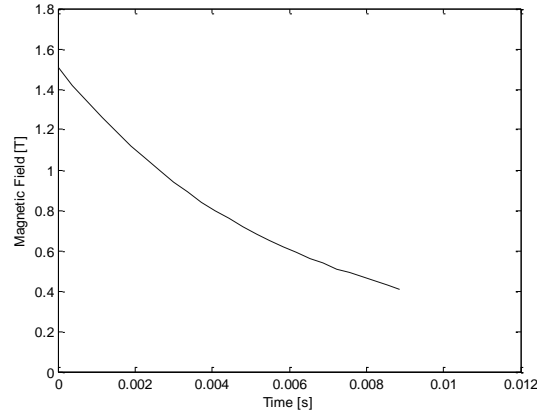


Figure 5: Magnetic field applied across the divergent section, in units of tesla, as a function of time.

The applied magnetic field must be reduced in time as the chamber pressure decays in order to maintain a constant exit Mach number for the present computation. The applied magnetic field shown in **Figure 5** maximizes the energy extracted while avoiding decelerating the flow to subsonic speeds. **Figure 6** shows the actual Mach number obtained at the nozzle exit on the basis of the applied magnetic field shown in **Fig. 5**.

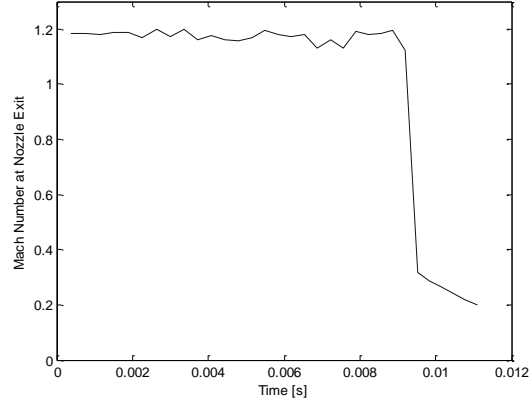


Figure 6: Nozzle exit Mach number as a function of time, computed from the blow-down model for the applied magnetic field shown in Fig. 5.

Note that at a time of about 9ms, a shock does enter the nozzle, indicated by the drop in the exit Mach number in **Fig. 6**. This shock is a result of a reduced dynamic pressure at the nozzle exit from the blow-down pressure decay and not a result of MHD application. The magnetic field is turned off when this shock occurs. This particular system operates at a relatively high ambient pressure and with a high exit-to-throat ratio. Both factors contribute to the formation of a shock. This will not occur with most other configurations.

The effect of the MHD generation/extraction on the Mach number within the nozzle flow is shown in **Figure 7**. At time $t = 2.3\text{ms}$, the plot shows Mach number, starting at the throat of the nozzle where the flow is sonic and ends at the nozzle exit. No MHD is applied in the first half of this section to allow the flow to be accelerated, since energy extraction at high velocities is beneficial. A spatially uniform magnetic field is applied to the downstream half of the diverging section, with temporal variation as shown in **Figure 5**. The energy extracted and drag created by the MHD generator lowers the Mach number. Without the MHD generator the flow would be accelerated to Mach ~ 4 , but the flow is only Mach 1.2 (by design) with the generation at the nozzle exit. This greatly reduces the impulse for the PDE, as momentum flux is the main component of thrust for this type of configuration. The Lorentz force and joule heating do raise the pressure in this divergent section, and at the exit at the time shown in **Fig. 7**, the exit pressure with MHD generation is 6 times higher than without the MHD. A lower exit Mach number increases the shock angle of the exhaust and increases the PDE's ability to have a shock travel into the bypass-tube.

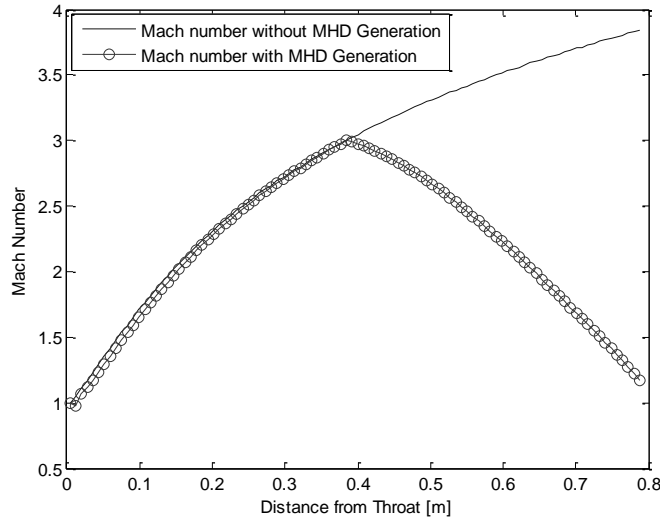


Figure 7: Mach number spatial evolution in the divergent section of the nozzle as a function of distance from the nozzle throat, at time 2.3ms. Results are shown for the PDE (blow-down model) with and without MHD generation in the region between 0.4 and 0.8m from the throat.

The six-fold exit pressure increase due to MHD generation is not enough to overcome the drag imparted on the system by the Lorentz force. **Figure 8** plots the overall impulse versus time with and without the MHD generation, as well as energy extracted (generated). There is a 40% loss of impulse due to the MHD generation in the nozzle for these conditions, but over 3 MJ may be extracted from this process for operation of the PDRIME.

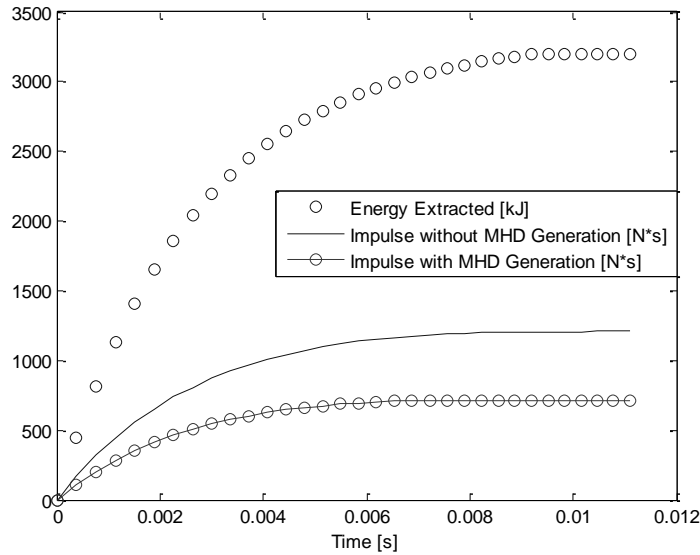


Figure 8: Energy extracted and impulse with and without MHD generation, plotted as a function of time, for the PDE (blow-down model).

The results of the PDE/blow-down model are then input into the bypass-tube model. There it can be determined whether this generated energy can be used to improve the net impulse of the system. This performance will be explored in a later section. At 6.8ms into blow-down, the chamber pressure is $1/10^{\text{th}}$ of its initial value. By this time, as seen in **Fig. 9**, nearly 100% of the impulse of this cycle has been produced and 95% of the energy has been generated. This is potentially a time at which the combustion chamber will start to be refilled with reactants.

The chamber pressure after a constant volume reaction is dependent on the pre-reaction pressure and temperature, assuming a fixed mass and volume. To achieve a ten-fold pressure increase during combustion, the

initial temperature of the reactants must be 300K. Higher pressure increases are created by lowering the initial temperature proportionally. The design trade-off is then average thrust versus required filling pressure. The total impulse of each cycle is relatively independent of the filling choice. However, filling at higher chamber pressures allows the filling process to start sooner, increasing the average thrust but requiring more elaborate pumping, something the basic PDE itself is supposed to avoid. At 10.8ms, the chamber pressure is reduced to $1/30^{\text{th}}$ of the initial value. A 30-fold pressure increase can be achieved with reactants filled at 100K. Depending on the application, this 4ms increase in blow-down time may be beneficial.

For every PDE configuration there are four important results to examine in the PDRIME concept. First, the impulse per cycle without MHD augmentation is recorded as a baseline. Next, both impulse per cycle with the MHD generation in the nozzle, as well as the energy generated, are also quantified. Lastly, the pressure at the exit of the nozzle is saved as a function of time.

The effect of the exit-to-throat area ratio and the altitude of operation for the PDRIME system may thus be explored for the PDE itself with a fixed combustion chamber geometry and an initial chamber pressure of 100atm. Cases with alternative initial chamber pressure conditions were run, as were cases with different chamber volumes while holding the initial chamber pressure constant. This latter instance increases the total mass of propellants used per cycle, but it makes little difference in specific impulse results. Initial combustion chamber pressure does have an impact on performance which is not fully explained by the proportional increase in propellant mass per cycle required to achieve it. This will be discussed further below. For the results in this section, the initial chamber pressure is held constant. Chamber pressure does proportionally change the nozzle exit pressure, of course.

Figure 9 plots the impulse per cycle of the PDE itself (via the blow-down model) for different values of the exit-to-throat area ratio and for different altitudes, without MHD generation and without the presence of the bypass tube. It should be noted that the ambient pressure is approximately halved with an altitude increase of 5km. At roughly ground level, where the ambient pressure is highest, the impulse is lowest due to the high drag ($P_a \gg P_e$ in equation 1). The optimal exit-to-area ratio for this altitude is five. Similar to constant-pressure rockets, as the ambient pressure is decreased, higher exit-to-throat area ratios are preferred, as the flow can be further expanded so as to equal the ambient pressure. At altitudes in excess of 15km, no maximum is achieved within this area ratio range. Due to the quasi 1-D approximation, momentum losses due to non-streamwise velocities are not accounted for. At large area ratios this will significantly reduce impulse. In addition, heavier nozzles required to achieve larger area ratios will counteract gains. These cycles all use 0.46kg of propellants. Here an impulse I of 1,000N*s corresponds to a specific impulse I_{sp} of 221s.

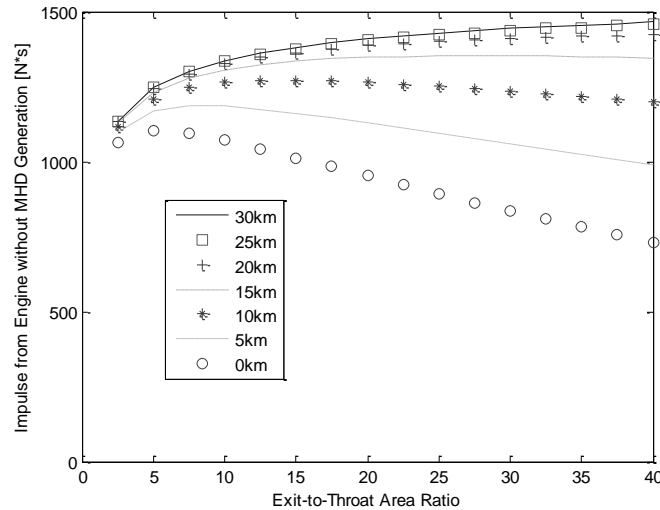


Figure 9: Total impulse as a function of exit-to-throat area ratio for various altitudes, for a single cycle PDE without MHD generation or augmentation.

MHD generation via a Lorentz force exerted on the propellant in the nozzle during energy extraction reduces the impulse of the engine system. **Figure 10** plots the impulse per cycle of the PDE, as a function of exit-to-throat ratio, with MHD generation in the nozzle's divergent section but without accounting for flow in the bypass tube. As seen in the figure, the greatest impulse reductions occur with the larger area ratios, due to the higher velocities and

larger areas over which MHD is applied. These factors also lead to a larger amount of energy being extracted from the flow.

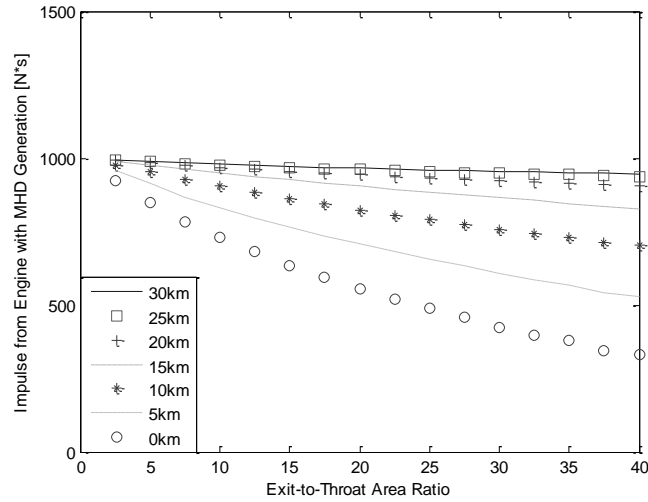


Figure 10: Impulse as a function of exit-to-throat area ratio for various altitudes for a PDE with MHD generation in the nozzle.

Figure 11 plots the energy generated by MHD in the nozzle as a function of nozzle exit-to-throat area ratio. The energy extracted in the nozzle strongly increases with increase exit-to-throat area ratio. Above 5km these are fairly independent of altitude. At lower altitudes the formation of shocks in the nozzle at high area ratios prematurely ends the energy extraction process. A comparison of energy generated per impulse lost, measured as the difference between impulse without and with MHD generation, yields approximately 6.3 [kJ/N*s] for all area ratios and altitudes.

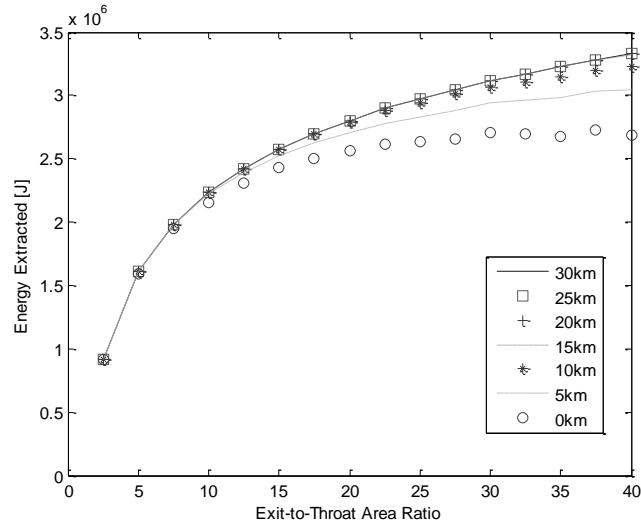


Figure 11: MHD energy generated in the nozzle as a function of exit-to-throat area ratio at different altitudes.

At higher altitudes (10 km and above), **Figure 11** shows the impulse per cycle is constant for a given area ratio. More energy is extracted at higher area ratios and this would appear to be the favorable configuration. However, this extra energy cannot be applied because of lower PDE nozzle exit pressures. **Figure 12** plots nozzle exit pressure versus time for different exit-to-throat area ratios at an altitude of 20km. The initial exit pressure for an area ratio of 2.5 is 9 times larger than for the area ratio 22.5 and 5 times greater than for the area ratio 12.5. In order to apply this extracted energy to the bypass-tube section, a shock must be produced to slow the flow in the bypass-tube. Low PDE nozzle exit pressures will not create strong enough (or any) shocks. All altitudes higher

than 20km will have identical exit pressure profiles, as the ambient pressure is too low to allow formation of a shock in the nozzle, which would disrupt blow-down. The results in **Fig. 13** suggest that lower nozzle area ratios could be more appropriate for PDRIME performance improvements.

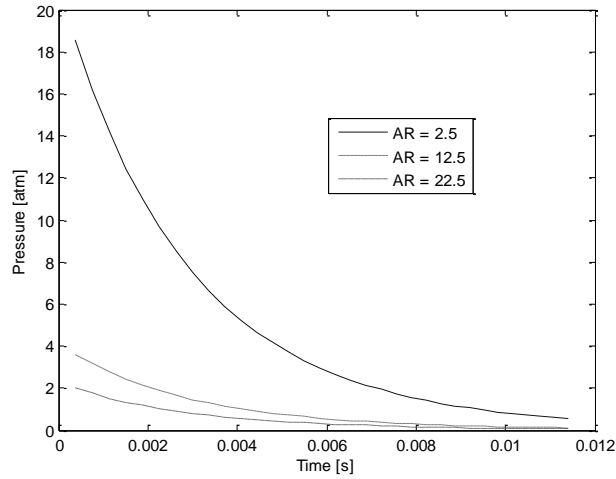


Figure 12. PDE nozzle exit pressure as a function of time for different exit-to-throat area ratios, with MHD generation in the nozzle.

For a given area ratio, the exit pressure can be proportionally increased by increasing the initial chamber pressure. Holding the post-reaction temperature in the chamber constant at 3000K dictates that an increase in initial chamber pressure also increases density proportionally. For all initial chamber pressures where nozzle shocks do not occur, energy extracted behaves identically as a function of area ratio when normalized by initial mass. While PDE impulse per cycle per mass does not behave the same for different initial chamber pressures at the same altitude, the values of specific impulse per cycle, for equal initial chamber to ambient pressure ratios, are equivalent. **Figure 13** plots the specific impulse, I_{sp} , per cycle for initial chamber pressures of 100 and 200 atm at several different altitudes, thus producing different chamber-to-ambient pressure ratios. This result allows quick estimates of extracted energy, impulse per cycle and exit pressure versus time to be obtained for different initial chamber pressures, information that allows computation of PDE impulse.

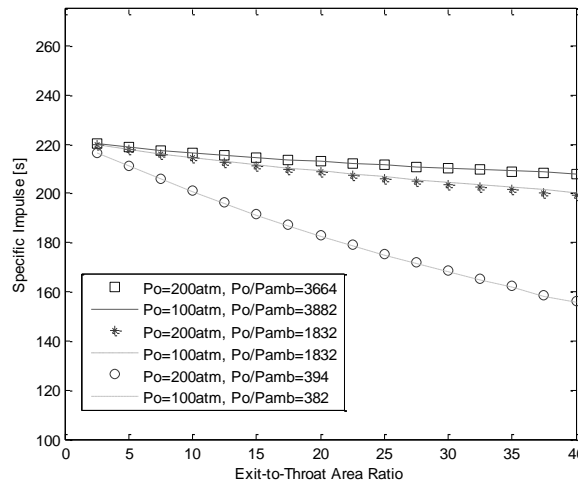


Figure 13. Specific impulse (I_{sp}) per cycle for different initial PDE chamber to ambient pressure ratios.

PDRIME Behavior

To study the overall PDRIME concept, PDE model results may be used as input for bypass-tube computations. The energy extracted from the PDE is used to power an MHD accelerator in the bypass-tube to create additional thrust. For this to be successful the exit pressure of the PDE has to be large enough to send a shock into

the bypass-tube. This shock must raise the temperature of the air in the bypass-tube above 3000K in order to be able to seed the air with Cesium. MHD can only be applied after the seeding increases the conductivity of the air. The performance of the whole system is analyzed.

As a 0th order approximation to this process, the pressure at the downstream end of the bypass-tube is set equal to the recorded PDE exit pressure. In reality the exhaust expands as it exits the PDE nozzle, reducing pressure, thus this 0th order approximation is clearly an over-estimation. The actual phenomena associated with shock transfer from the nozzle to the bypass section are explored separately using 2D transient WENO simulations, discussed later. For now, the best case scenario is assumed. This allows for the validity of this method of augmentation to be shown and important trends to be identified.

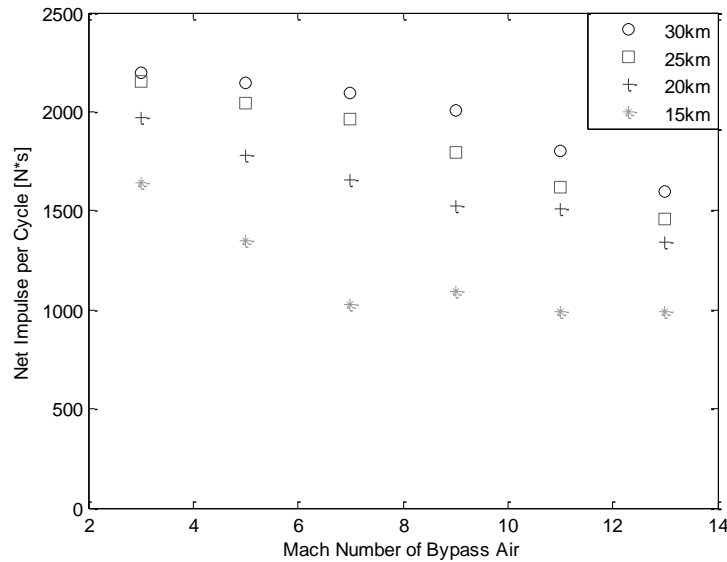


Figure 14: Net impulse of the PDRIME cycle as a function of bypass air Mach number at different altitudes for an exit-to-throat area ratio of 2.5 with a bypass-tube area of 0.09m².

Figure 14 plots the net impulse per cycle of the PDRIME system with an exit-to-throat area ratio of 2.5. Each set of similar marks represent a single PDRIME operating at a fixed altitude at different flight Mach numbers. A net impulse of 2,200N*s is achieved at two different altitudes. One set of operating conditions where this is achieved is at an altitude of 25km where the vehicle is traveling at Mach 3 (the inlet Mach number for the bypass tube). This corresponds to a specific impulse of 489s, more than a 60% increase in impulse over any non-augmented PDE configuration with the same geometry, and shows potential for the PDRIME concept.

There are several factors which contribute to the range of inlet Mach numbers and altitudes for which the PDRIME will be effective. Low flight Mach numbers lead to lower temperatures behind the bypass-tube shock, making thermal ionization impossible. Yet large flight Mach numbers cause the total pressure to become too large, and no shock can enter the bypass-tube. Lower altitudes have the negative effects of not allowing shocks to enter the bypass-tube and reducing the temperature behind the shock, due to the lower pressure ratio across the shock. At altitudes below 15km the PDRIME system does not appear to be viable.

If the exit pressure of the PDE nozzle is too low, no combination of altitude and Mach number can be successful. Even if a shock can be formed in the bypass section, it will not generate the require temperature gain. **Figure 15**, for example, plots the net impulse per cycle of the PDRIME system for only the PDE portion with an exit-to-throat area ratio of 7.5, producing a high Mach number and relatively low pressure at the nozzle exhaust; the resulting impulse is over a factor of two below that for the nozzle with area ratio 2.5, shown in **Fig. 14**.. This illustrates the tremendous vulnerability of this system and its need for high nozzle exit pressure. Even when assuming no pressure loss or expansion as the shock travels from the nozzle exit to the downstream end of the bypass section, the net impulse is relatively low; the system is in fact ineffective for exit-to-throat areas exceeding 5.

Weak exit pressures reduce total net impulse in three main ways. First, the lower pressures fail to keep the shock in the bypass-tube at higher Mach numbers. Second, the lowered pressure ratio results in less of a temperature jump across the shock entering the bypass section, making seeding difficult. Third, the velocity of the

air behind the bypass-tube shock is higher for lower pressures across the entering shock. These higher velocities in the tube require more energy to be applied to produce the same addition impulse.

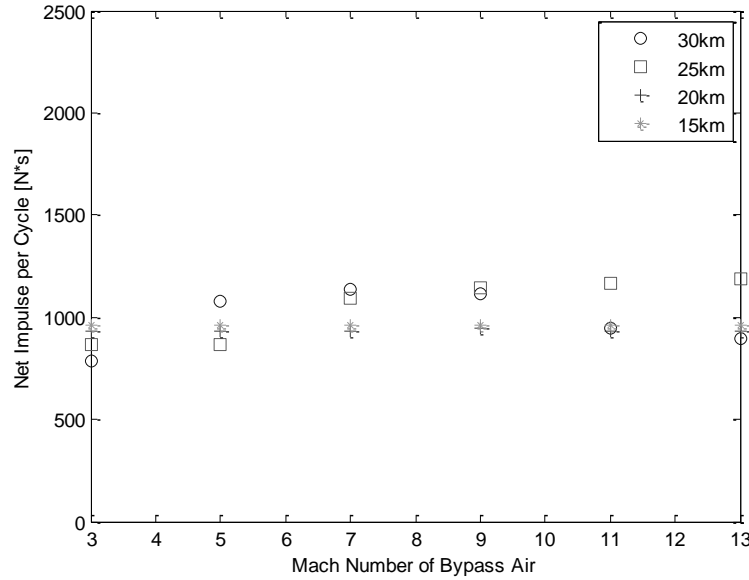


Figure 15: Net impulse of the PDRIME cycle as a function of bypass air Mach number at different altitudes for an exit-to-throat area ratio of 7.5 with a bypass-tube area of 0.09m^2 .

The effect of the cross-sectional area of the bypass-tube is now considered. First this will be examined while maintaining the pressure match between the exit of the PDE nozzle and the exit of the bypass-tube. **Figure 16** plots the net impulse of the PDRIME cycles at an altitude of 25km for different cross-sectional areas of the bypass-tube. There is a clear trend indicating that the higher the bypass-tube area, the greater the net impulse of the cycle. Recall that the energy applied is proportional to velocity squared. When MHD acceleration is applied, a Lorentz force is exerted on the air in the nozzle as an equal and opposite force to that which acts on the bypass-tube magnets providing thrust. If the bypass-tube area is large, most of the energy can be applied before the air is accelerated to very high velocities where MHD acceleration becomes expensive.

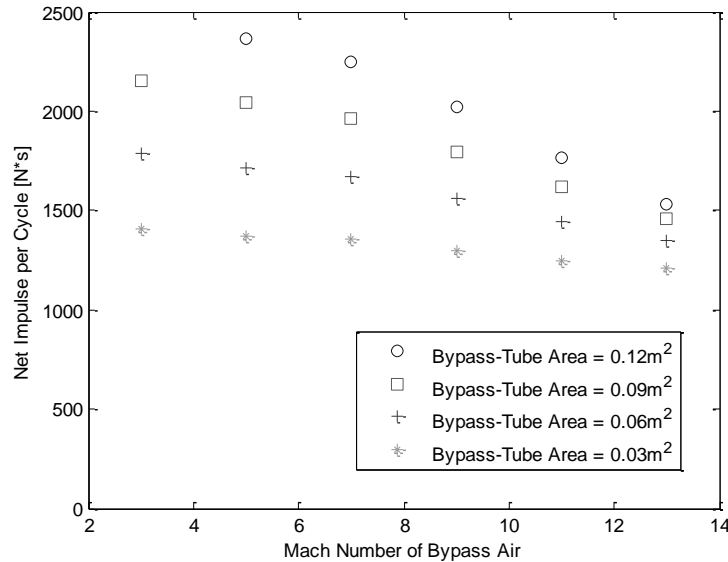


Figure 16: Net impulse of the PDRIME cycle as a function of bypass air Mach number at different bypass-tube areas for an exit-to-throat area ratio of 2.5 at an altitude of 25km, assuming no shock pressure losses associated with flow from the nozzle exit to the bypass exit.

The exit area of the PDE used in **Figure 17** is 0.06m^2 . The ability of the nozzle exhaust to send a shock into the bypass-tube will surely be a function of the bypass-tube cross-sectional area. To put a theoretical limit on the bypass-tube area, the energy of the exhaust flow may be quantified. The exit pressure for the quasi-1D simulation represents the entire pressure across the nozzle exit. If this is viewed as a type of energy density, when the exhaust leaves the nozzle and expands vertically across the bypass-tube exit, the maximum pressure that can be present at the bypass-tube exit could be considered to be the “new” energy density, which accounts for this expansion via the relation:

$$p_{by} = \left(\frac{A_e}{A_e + A_{by}} \right) \cdot p_e \quad (18)$$

where p_{by} is the pressure applied to the exit of the bypass-tube accounting for the bypass section’s cross-sectional area, A_{by} , and the nozzle exhaust area, A_e . This expression is still an over-estimation of the pressure at the bypass tube exit because it assumes uniform pressure in the transition from the center of the nozzle exit to the top of the bypass-tube. **Figure 17** shows the variation in net impulse for the PDRIME as a function of flight Mach number for different bypass tube cross-sectional areas. In comparison with the more idealized performance shown by the results in **Figure 16**, there is a considerable drop in impulse, in some cases by a factor of two. It is clear that the benefits of larger bypass-tube areas are canceled by the more realistically low average pressure across the tube’s exit.

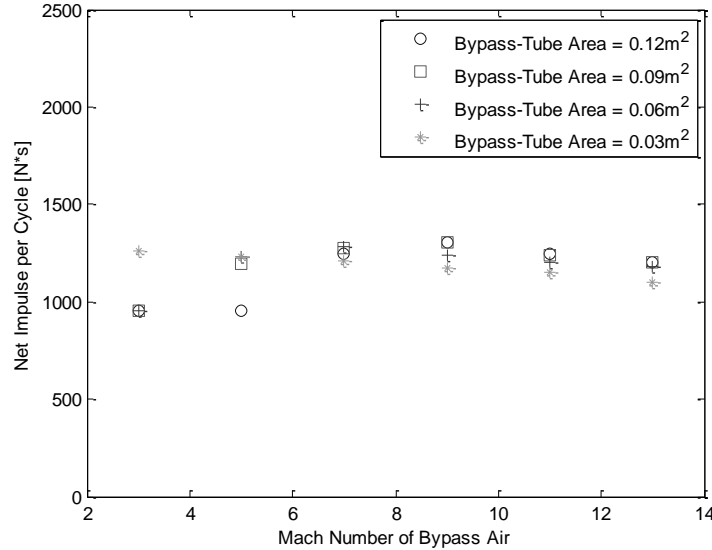


Figure 17: Net impulse of the PDRIME cycle as a function of bypass air Mach number at different bypass-tube areas for an exit-to-throat area ratio of 2.5 at an altitude of 25km, accounting for expansion pressure losses via eqn. (18).

As noted previously, a comparison of results from the present simplified blow-down model and quasi 1D nozzle and bypass tube simulations to represent the PDRIME configuration may be made with a more realistic, 2D transient simulation of nozzle, external flow, and bypass tube flow and MHD processes. The transmission of the shock from the nozzle exit to the end of the bypass tube is one obvious phenomenon to explore, given the approximations leading to the differing results in **Figures 16 and 17**. Using the 2D transient simulation, it is observed that, for the PDRIME configuration with a nozzle area ratio of 2.5 operating at Mach 5 and at an altitude of 30 km, the shock exiting the nozzle does propagate into the bypass tube and travel upstream. But it is observed in this case that the temperature in the bypass section does not exceed 3000K, a requirement for ionizing seeded Cesium in the tube. Hence a slightly altered PDRIME geometry, one where the upper wall is extended by 0.5 m, is considered. This altered system allows the shock to be directed and captured more fully into the bypass tube, and correspondingly allows the temperature there to increase, exceeding 3000K. A comparison of the temperature fields at the same time for both configurations is shown in **Figure 18**. Since the presence of the upper wall would not have

an effect in the idealized, inviscid quasi 1D model results, the configuration with the extended upper wall will be used in the 2D simulations for further comparisons.

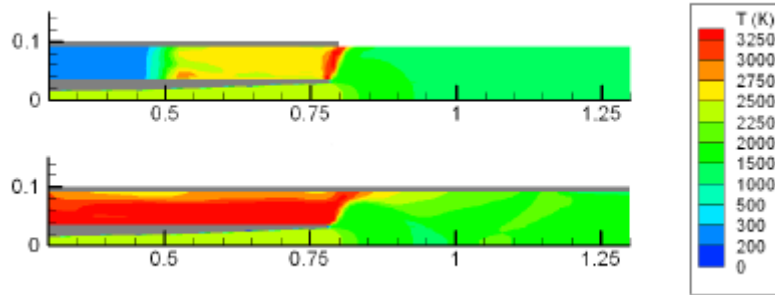


Figure 18: 2D temperature field contours for the upper part of the PDE section and the bypass section, at a time $t = 1.0$ ms after the start of the blowdown process. Both images show a PDRIME geometry with MHD generation in the nozzle but without energy application in the bypass section, but the lower image has a 0.5 m extension to the upper wall of the bypass section; the upper image does not. The flight Mach number is 5, the nozzle area ratio is 2.5 and the bypass section cross-sectional area is 0.06 m^2 .

Figures 19 and 20 show the predicted evolution of the pressure and temperature fields, respectively, for the PDRIME with MHD generation in the nozzle and with energy application in the bypass tube, for a geometry that includes the bypass upper wall extension. A shock structure is observed to transition from the nozzle to the bypass tube before being forced back downstream under the influence of both the Mach 5 inlet flow and the MHD accelerator.

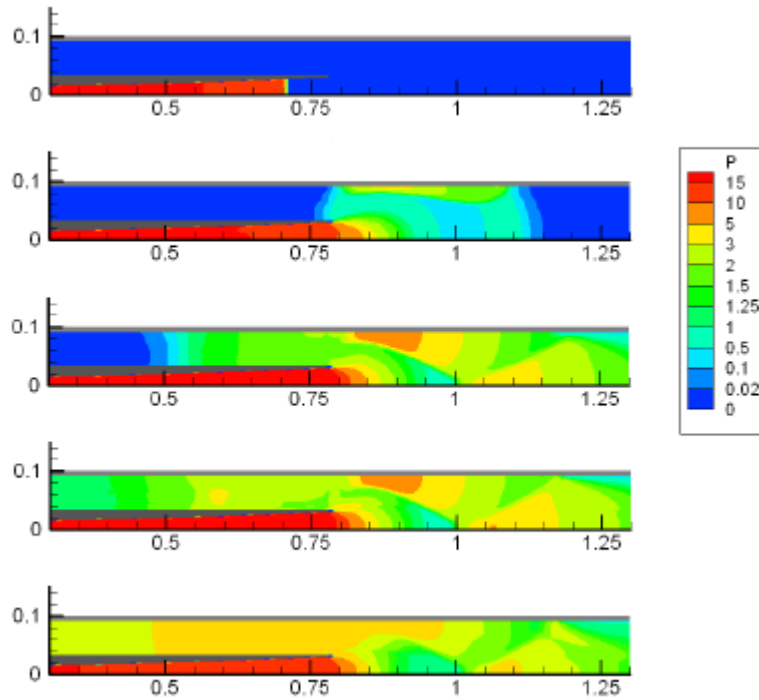


Figure 19: 2D pressure (in atm) field contours for the upper part of the PDE section and the bypass section, at different times after the start of the blowdown process (top to bottom, $t = 0.0, 0.1$ ms, 0.5 ms, 1.0 ms, and 2.0 ms). Results are for a PDRIME geometry with MHD generation in the nozzle and with energy application in the bypass section. The flight Mach number is 5, the nozzle area ratio is 2.5 and the bypass section cross-sectional area is 0.06 m^2 .

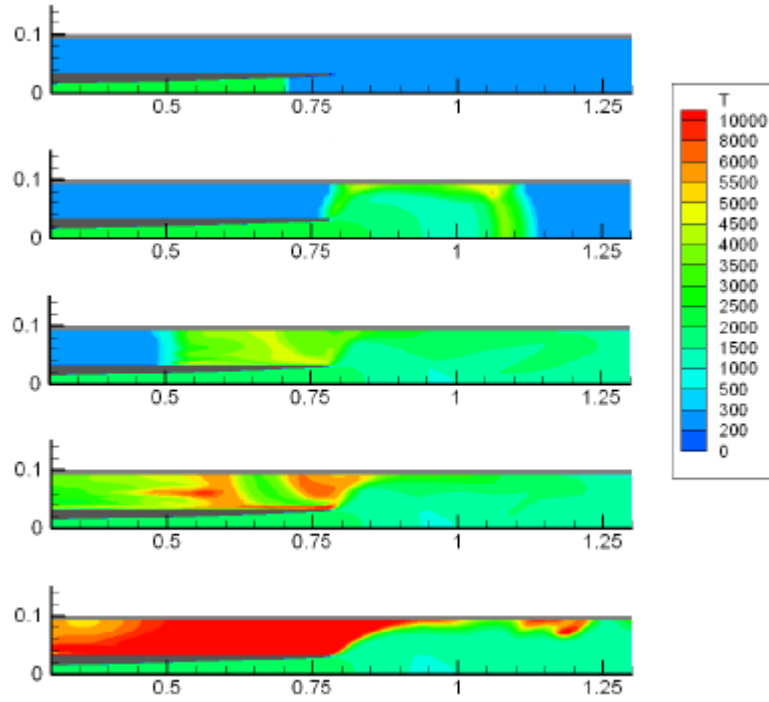


Figure 20: 2D temperature (in K) field contours for the upper part of the PDE section and the bypass section, at different times after the start of the blowdown process (top to bottom, $t = 0.0, 0.1$ ms, 0.5 ms, 1.0 ms, and 2.0 ms). Results are for a PDRIME geometry with MHD generation in the nozzle and with energy application in the bypass section. The flight Mach number is 5, the nozzle area ratio is 2.5 and the bypass section cross-sectional area is 0.06 m^2 .

The temperature plot in **Fig. 20** illustrates a small sliver of high-temperature fluid appearing briefly along the inside wall of the bypass, a result of the vertical Lorentz forces accelerating the fluid upward and producing a small low-density region. In reality, viscous forces would prevent this region from forming, while the artificial dissipation inherent to the WENO numerical scheme is likely over-estimating the associated temperature. Since this is an inviscid simulation and since artificial dissipation is necessary for properly capturing shocks, we prevent the temperature from rising to unrealistic degrees by setting the accelerator to induce force on a fluid cell only if its temperature lies below 20000K. The nozzle/bypass exit pressure evolution indicates that after the bypass has begun pushing back the shock, the bypass tube exit pressure p_{by} is roughly half of the nozzle exit pressure, which is consistent with the approximation in eqn. (18). Yet at the earlier stages of the cycle, this loss factor is below the value predicted by eqn. (18).

Although there are clearly differences in the flow evolution between the quasi 1D idealized model and the 2D flow in the actual configuration, especially between the nozzle exit and the bypass tube, the ultimate difference in PDRIME total impulse is not very large. **Table 1** shows differences between the simplified model results for impulse and those derived for the same geometry and conditions from the 2D simulation. For the case without MHD acceleration in the bypass tube, impulse is computed only on the basis of a control volume enclosing the PDE itself. For the case without MHD generation or acceleration, the impulse differs only slightly between the two simulations. When MHD generation in the nozzle takes place but without MHD acceleration in the bypass section (“Gen only” in **Table 1**), there appears to be about a 10% difference between the quasi 1D and 2D simulation results. Yet this may be because the effect of the Lorentz force and associated transient term in the momentum flux in the divergent section of the nozzle was neglected in the quasi 1D simulations due to the quasi-steady nature of the model in that location. When this effect is removed in the 2D simulations, the computed impulse is closer to that predicted by the quasi 1D simulation. When both MHD generation and application of energy in the bypass section take place (“Gen + 1 Byp” in **Table 1**), there are more significant differences between the two methods, yielding nearly an 18% reduction in impulse when going from the quasi 1D to the 2D simulations. Moreover, with the more “realistic” 2D flow simulation, there is actually a reduction in impulse seen between the conditions without MHD and with MHD, in contrast to the improvement in impulse observed by the quasi 1D simulation. On the other hand,

when a second bypass tube is employed in the 2D simulations, below the PDE (thus creating a symmetric configuration), there is a 10% improvement in overall impulse observed, as suggested by the “Gen + 2 Byp” result in **Table 1**. Splitting the energy extracted from the PDE nozzle between bypass-tubes above and below the PDE allow the energy to be applied at low velocities, effectively doubling the bypass-tube area without reducing the pressure by its exit. Additional 2D computations described by Zeineh¹⁹ suggest that the presence of a “magnetic piston” in the chamber, in addition to the PDRIME bypass configuration, can yield further increases in impulse, that is, when energy extraction from the nozzle is used to accelerate flow in the bypass section as well as to accelerate products out of the combustion chamber. Further exploration of these alternative MHD thrust augmentation concepts is ongoing.

Config	AR=2.5	AR=2.5
-	Quasi-1D	2D
No MHD	1135	1120
Gen Only	995	897
Gen + 1 Byp	1227	1011
Gen + 2 Byp	-	1134

Table 1. Comparison of total impulse (units of N-sec) computed from the simplified PDRIME model and the 2D transient simulation. Results are shown for the case without any MHD generation or acceleration in the bypass tube, for the case of MHD generation/extraction in the nozzle, and for MHD generation and energy application in the bypass tube.

Discussion and Conclusions

The present simulations do suggest that the PDRIME system shows potential for an increase in both impulse and specific impulse. A possible 60% increase in these performance parameters is observed under idealized, optimal conditions (e.g., at altitudes around 25 km with a relatively large bypass tube cross-sectional area and at a flight Mach number around 5). This improved performance is achieved, however, under the assumption of matching pressure in the nozzle exit and the bypass-tube exit. Under the still idealized energy density conditions assumed via eqn (18) for the area difference between the nozzle exit and the bypass tube, the net improvement is greatly decreased, but comparisons with full 2D simulations suggest that this reduced performance may be a reasonable approximation for actual performance (within 20%).

The potential benefits of the PDRIME system are mainly seen for low exit-to-throat area ratios, 2.5, due to the reduction in exit pressure from further expansion. Yet the impulse gained by the PDRIME system is strongly dependent on the area of the bypass-tube and the exit pressure applied to its exit. With the idealization of the nozzle exit pressure boundary condition applied to the bypass-tube held constant, larger areas lead to larger impulse improvements, due to the larger amount of energy which can be applied before this acceleration brings the bypass air to high velocities. The bypass-tube area is limited by the decrease in average pressure which occurs as its cross-sectional area is increased. This relationship between average pressure and area makes this concept seem unlikely to create great improvement in net impulse over standard PDEs with larger area ratios. On the other hand, this concept may be able to provide modest impulse gains at high altitudes. At low altitudes the MHD energy transfer mechanisms can be disengaged. Due the low area ratio required for the PDRIME, drag as a result of high ambient pressure could be mitigated. The PDRIME system would thus be best suited for low and high altitude flight.

The PDRIME concept may achieve more of its high potential by inventive methods for increasing the pressure at the exit of the bypass-tube. One method is a extending the top wall of the bypass-tube to trap the nozzle exit, as shown in **Fig. 18** and subsequent images, or by employing a second bypass tube, or by also employing a magnetic piston, all of which are being explored by Zeineh¹⁹. There are thus a range of alternative configurations to explore in assessing the benefits of MHD thrust augmentation for propulsive devices.

PREPRINT

Acknowledgments

The authors wish to acknowledge the technical assistance of Dr. Xing He of the UCLA Department of Radiological Sciences in performing the 2D transient simulations, and by Mr. Lord Cole of the UCLA MAE Department in performing the quasi 1D simulations described in this work. This research has been supported at UCLA by the Air Force Office of Scientific Research under the space power and propulsion program managed by Dr. Mitat Birkan (Grants FA9550-07-1-0156 and FA9550-07-1-0368). Grant management by Dr. Andrew Ketsdever of the Air Force Research Laboratory at Edwards, CA (AFRL/RZSA) is also gratefully acknowledged.

References

- ¹ J.-L. Cambier, "MHD Augmentation of Pulse Detonation Rocket Engines", 10th Intl. Space Planes Conf., Kyoto, Japan, April 2001, AIAA paper 2001-1782.
- ² Hill, P. and Peterson, C., **Mechanics and Thermodynamics of Propulsion**, 2nd Edition, Addison-Wesley publishing company, 1992.
- ³ Kailasanath, K., and Patnaik, G., "Performance Estimates of Pulse Detonation Engines," *Proceedings of the Combustion Institute*, Vol. 28, 2000, pp. 595–602.
- ⁴ Cooper, M., and Shepherd, J. E., "The Effect of Nozzles and Extensions on Detonation Tube Performance", AIAA paper 02-3628, 38th AIAA/ASME/SAE/ASEE Joint Propulsion Conference, July, 2002.
- ⁵ Cooper, M. and Shepherd, J. E., "Single Cycle Impulse from Detonation Tubes with Nozzles", *Journal of Propulsion and Power*, Vol.24 no.1, 2008, pp. 81-87.
- ⁶ Eidelman, S., Grossmann, W., and Lottati, I., "Review of Propulsion Applications and Numerical Simulations of the Pulse Detonation Engine Concept," *Journal of Propulsion and Power*, Vol. 7, No. 6, 1991, pp. 857–865.
- ⁷ Wintenberger, E., Austin, J. M., Cooper, M., Jackson, S., and Shepherd, J. E., "An Analytical Model for the Impulse of a Single Cycle Pulse Detonation Engine," *Journal of Propulsion and Power*, Vol. 19, No. 4, 2003, pp. 22–38; also *Journal of Propulsion and Power*, Vol. 20, No. 4, 2004, pp. 765–767.
- ⁸ Li, C., and Kailasanath, K., "Partial Fuel Filling in Pulse Detonation Engines," *Journal of Propulsion and Power*, Vol. 19, No. 5, 2003, pp. 908–916.
- ⁹ Warwick, G., "U.S. AFRL proves pulse-detonation engine can power aircraft", Flight Magazine, March 5, 2008 (online at <http://www.flightglobal.com/articles/2008/03/05/222008/us-afrl-proves-pulse-detonation-engine-can-power-aircraft.html>).
- ¹⁰ He, X. and Karagozian, A. R., "Numerical Simulation of Pulse Detonation Engine Phenomena", *Journal of Scientific Computing*, Vol. 19, Nos. 1-3, pp.201-224, December, 2003.
- ¹¹ He, X. and Karagozian, A. R., "Pulse Detonation Engine Simulations with Alternative Geometries and Reaction Kinetics", *Journal of Propulsion and Power*, Vol. 22, No. 4, pp. 852-861, 2006.
- ¹² Harten, A., Osher S. J., Engquist, B. E., and Chakravarthy, S. R., "Some Results on Uniformly High-Order Accurate Essentially Nonoscillatory Schemes", *J. Appl. Numer. Math.*, Vol. 2, pp. 347-377, 1986.
- ¹³ Jiang, G. S. and Shu, C. W., "Efficient Implementation of Weighted ENO Schemes", *Journal of Computational Physics*, Vol. 126, pp. 202-228, 1996.
- ¹⁴ J.-L. Cambier, "A Thermodynamic Study of MHD Ejectors", AIAA paper 98-2827, 34th AIAA/ASME/SAE/ASEE Joint Propulsion Conference, July, 1998.
- ¹⁵ Hwang, P., Fedkiw, R. P., Merriman, B., Aslam, T. D., Karagozian, A. R., and Osher, S. J., "Numerical Resolution of Pulsating Detonation Waves", *Combustion Theory and Modelling*, Vol. 4, No. 3, pp. 217-240, September, 2000.
- ¹⁶ Henrick, A. K., Aslam, T. D., and Powers, J. M., "Mapped Weighted Essentially Non-oscillatory Schemes: Achieving Optimal Order near Critical Points," *Journal of Computational Physics*, Vol. 207, No. 2, 2005, pp. 542–567.
- ¹⁷ J.-L. Cambier, "Preliminary Model of Pulse Detonation Rocket Engines", 35th AIAA/ASME/SAE/ASEE Joint Propulsion Conference, Los Angeles, June 1999, AIAA paper 1999-2659.
- ¹⁸ Shu, C. W., and Osher, S., "Efficient Implementation of Essentially Non-Oscillatory Shock Capturing Schemes II", *Journal of Computational Physics*, Vol. 83, pp. 32-78, 1989.
- ¹⁹ Zeineh, C., "Numerical Simulation of Magnetohydrodynamic Thrust Augmentation for Pulse Detonation Rocket Engines", Ph.D. prospectus, UCLA Department of Mechanical and Aerospace Engineering, 2008.